Oligopeptidase B: A New Type of Serine Peptidase with a Unique Substrate-Dependent Temperature Sensitivity†

László Polgár*

Institute of Enzymology, Biological Research Center, Hungarian Academy of Sciences, P.O. Box 7, Budapest H-1518 Hungary

Received July 29, 1999; Revised Manuscript Received September 14, 1999

ABSTRACT: Oligopeptidase B, a member of the novel prolyl oligopeptidase family of serine peptidases, is involved in cell invasion by trypanosomes. The kinetic analysis of the reactions of oligopeptidase B, which preferentially cleaves peptides at two adjacent basic residues, has revealed significant differences from the trypsin-like serine peptidases. (i) The pH dependence of k_{cat}/K_m deviates from normal bell-shaped curves due to ionization of an enzymatic group characterized by a macroscopic pK_a of ~8.3. The effect of this group is abolished at high ionic strength. (ii) The second-order acylation rate constants, k_{cat}/K_m, are similar with the ester and the corresponding amide substrates, suggesting that their chemical reactivity does not prevail in the rate-limiting step. The kinetic deuterium isotope effects indicate that the rate-limiting step for k_{cat}/K_m is principally governed by conformational changes. (iii) The pH−k_{cat}/K_m profile and the very low rate constant for benzoyl-citrulline ethyl ester reveal a new kinetically influential group ionizing below the pK_a of the active site histidine and indicate that the positive charge of arginine is essential for effective catalysis. (iv) The enzyme is inhibited by high concentrations of substrate. The mechanism of inhibition markedly varies with the reaction conditions. (v) The optimum temperature for the reactions of amide substrates is unusually low, slightly below 25 °C, whereas with benzoyl-arginine ethyl ester a linear Eyring plot is obtained up to 39 °C. The positive entropies of activation point to substantial reorganization of water molecules upon substrate binding.

In addition to the extensively studied trypsin and subtilisin families, a new class of serine peptidases has recently been identified and called the prolyl oligopeptidase family (*1*). The members of the new family exhibit much larger molecular masses (about 80 kDa) with respect to trypsin and subtilisin and have a single polypeptide chain, displaying the peptidase domain at the C-terminus. The catalytic domain of the members of the prolyl oligopeptidase family is structurally related to lipases rather than to peptidases (*2*). Detailed kinetic investigations have only been carried out with prolyl oligopeptidase, the prototype of the family (cf. *3* and references therein).

The three-dimensional structure of prolyl oligopeptidase has also been determined (*4*). The enzyme contains two domains. The catalytic domain shows a twisted eight-stranded β-sheet which is flanked with several helices. The other domain is an unusual seven-bladed β-propeller, which exhibits a 7-fold repeat of four-stranded antiparallel β-sheets. The seven blades of the propeller are twisted and radially arranged around their central tunnel. In contrast to the previously determined propellers, the oligopeptidase domain is not closed between the first and last blades. This may allow oligopeptides to enter the cavity of the enzyme and excludes large peptides and proteins from the active site. The catalytic triad (Ser554, Asp641, and His680) is located at the interface of the two domains.

Oligopeptidase B (EC 3.4.21.83), previously called protease II, is homologous to prolyl oligopeptidase (*5*, *6*). It was first isolated from *Escherichia coli* cells with trypsin-like specificity, cleaving peptides at lysine and arginine residues (cf. *7*). We have recently shown that oligopeptidase B hydrolyzes peptides with dibasic sites much faster than monobasic substrates (*8*). The k_{cat}/K_m for Z-Arg-Arg-Amc[1] is extremely high, 63 $\mu M^{-1} s^{-1}$, and this preference for adjacent arginine residues indicates that oligopeptidase B may be a new type of processing enzyme. The catalytic triad (Ser, His, Asp) of oligopeptidase B, as well as that of prolyl oligopeptidase, is distinct from that of the trypsin and subtilisin type enzymes, as indicated by ^{1}H NMR studies demonstrating that the high-frequency, low-barrier hydrogen bond between the Asp and His residues, a universal trait of the well-known serine peptidases, is absent in free prolyl oligopeptidase and oligopeptidase B (*9*).

Oligopeptidase B is also present in *Trypanosoma* cruzi, the causative agent of Chagas' disease in humans. It is implicated in the host cell invasion by the parasite by generating an active Ca^{2+} agonist from a cytosolic precursor molecule (*10*, *11*). The present paper reports several mechanistic features of oligopeptidase B different from those of

† This work was supported by OTKA T/11 (Grant (T029056), the Royal Society Joint Projects with Central and Eastern Europe, and the Wellcome Collaborative Research Initiative Grant (no. 055178/Z/97/Z/98/Z).

* To whom correspondence should be addressed. Fax: 36-1-466-5465. E-mail: polgar@hanga.enzim.hu.

[1] Abbreviations: DMF, dimethylformamide; EDTA, ethylenediaminetetracetic acid; Mes, 2-(morpholino)ethanesulfonic acid; Cit, citrulline; Z, benzyloxycarbonyl; Bz, benzoyl; Nan, 4-nitroanilide; Nap, β-naphthylamide; Amc, 7-(4-methylcoumaryl)amide; Et, $-OC_2H_5$.

10.1021/bi991767a CCC: $18.00
Published on Web 11/03/1999

trypsin and prolyl oligopeptidase, and this can help in the design of inhibitors against the enzyme to counteract the parasite.

EXPERIMENTAL PROCEDURES

Enzyme. Oligopeptidase B was overexpressed in *E. coli* cells, purified, and assayed as described (*12*). The concentration of the enzyme was determined at 280 nm, using a molecular mass of 81 858 kDa and A_{280} of 1.83 for the 1.0 mg/mL concentration (*12*).

Kinetics. The specificity rate constants (k_{cat}/K_m) were determined under first-order conditions, i.e., at substrate concentrations lower than K_m. The first-order rate constant was divided by the total enzyme concentration to provide k_{cat}/K_m. For the determination of the rate constant, the stock solution of Bz-Arg-Nan (4 mg/mL in DMF) was diluted 40-fold (230 μM) with water, and 20 μL of this solution was added to the reaction mixture with a 1.0 mL final volume. The reactions were measured with a Cary 1E spectrophotometer at 400 nm in a four-component buffer, which consisted of 25 mM glycine, 25 mM acetic acid, 25 mM Mes, and 75 mM Tris and contained 1 mM EDTA (standard buffer). The buffer was titrated to the desired pH with HCl or NaOH, while the ionic strength remained fairly constant over a wide pH range. Small changes in the conductivity were adjusted by the addition of NaCl.

The Michaelis parameters were determined with initial rate measurements. To eliminate high concentrations of DMF when working at elevated Bz-Arg-Nan concentrations, the substrate was freshly dissolved in 20 mM Tris buffer of appropriate pH (2 mg/mL). The hydrolysis of Bz-Arg-Nap was monitored fluorometrically at 25 °C by using a Jasco FP 777 spectrofluorometer equipped with a thermostated cell holder. The excitation and emission wavelengths were 340 (1.5 nm bandwidth) and 410 nm (5 nm bandwidth), respectively. The hydrolyses of Bz-Arg-NH_2, Bz-Arg-Et, and Bz-Cit-Et at concentrations between 20 and 50 μM were measured at 253 nm with a Cary 1E spectrophotometer equipped with a thermostated cell holder.

Theoretical curves for bell-shaped pH−rate profiles were calculated by nonlinear regression analysis, using eq 1 and the GraFit software (*13*). In eq 1, k_{cat}/K_m(limit) stands for

$$k_{cat}/K_m = k_{cat}/K_m(\text{limit})[1/(1 + 10^{pK_I - pH} + 10^{pH - pK_{II}})] \quad (1)$$

the pH-independent maximum rate constant and K_I and K_{II} are the dissociation constants of a catalytically competent base and acid, respectively. At low ionic strength, an additional ionizing group modifies the bell-shaped character of the pH dependence curve. The resulting pH-rate profile conforms to eq 2, where the limiting values stand for the pH independent maximum rate constants for the two active forms of the enzyme and K_1, K_2, and K_3 are the dissociation constants of three enzymatic groups whose state of ionization controls the rate constants. The pH-rate profile for Bz-Cit-Et in 1.0 M NaCl was calculated by using eq 3.

$$k_{cat}/K_m = k_{cat}/K_m(\text{limit})_1[1/(1 + 10^{pK_1 - pH} + 10^{pH - pK_2})] + k_{cat}/K_m(\text{limit})_2[1/(1 + 10^{pK_2 - pH} + 10^{pH - pK_3})] \quad (2)$$

$$k_{cat}/K_m = k_{cat}/K_m(\text{limit})[1/(1 + 10^{pK_1 - pH} + 10^{pH - pK_2})] + k_{cat}/K_m(\text{limit})_2[1/(1 + 10^{pK_2 - pH})] \quad (3)$$

When two substrate molecules bind to the same enzyme molecule and this generates an inactive complex, the Michaelis parameters cannot be determined by the conventional methods. In such a case, eq 4 applies, where K_{is} is the second dissociation constant of the inhibited enzyme−substrate complex (*14*).

$$v = V[S]/(K_m + [S] + [S]^2/K_{is}) \quad (4)$$

The K_i, which is different from K_{is} of eq 4, represents the dissociation constant of the enzyme−inhibitor complex measured with a relatively poor substrate as the inhibitor. It was calculated from a plot of k_i/k_0 vs inhibitor concentration, using eq 5, where k_0 and k_i are pseudo-first-order rate constants for the hydrolysis by the highly specific substrate, Z-Arg-Arg-Amc, in the absence and presence of inhibitor (I), respectively. The Z-Arg-Arg-Amc concentration was at least 10-fold less than K_m, and thus K_i represents a true dissociation constant of the enzyme−substrate/inhibitor complex.

$$k_i/k_0 = 1/(1 + [I]/K_i) \quad (5)$$

The temperature dependence of the rate constants was determined in thermostated cell holders. The reactions were started after the thermal equilibrium had been reached in the cell, which was checked with a Digi-Sense thermometer (Cole-Palmer). Activation parameters were calculated from the linear plots of ln(k/T) versus $1/T$ (eq 6), where k is the rate constant, R is the gas constant (8.314 J/mol/K), T is the absolute temperature, N_A is Avogadro's number, h is Planck's constant, the enthalpy of activation $\Delta H^* = -$(slope)8.314 J/mol, the entropy of activation $\Delta S^* =$ (intercept − 23.76)8.314 J/mol/K. The free energy of activation, ΔG^*, was calculated from eq 7.

$$\ln(k/T) = \ln(R/N_A h) + \Delta S^*/R - \Delta H^*/RT \quad (6)$$

$$\Delta G^* = \Delta H^* - T\Delta S^* \quad (7)$$

Rate-limiting general acid/base catalysis was tested in heavy water (99.9%). The deuterium oxide content of the reaction mixture was at least 95%. The p^2H of a deuterium oxide solution can be obtained from pH meter reading according to the relationship p^2H = pH(meter reading) + 0.4 (*15*).

The thiol groups of oligopeptidase B were reacted with 1 mM iodoacetamide for 12 h at 25 °C. The thiol content of the enzyme was determined with 5,5′-dithiobis(2-nitrobenzoic acid) (*16*).

RESULTS AND DISCUSSION

Effects of Organic Solvents. The synthetic substrates of peptidases are often dissolved in organic solvent, which may markedly inhibit the catalytic activity, as found with prolyl oligopeptidase, a close relative of oligopeptidase B (*3*). Such an effect can also be observed in the reaction of oligopeptidase B with Bz-Arg-Nan. As seen in Figure 1, the inhibition with increasing DMF concentration follows a single-

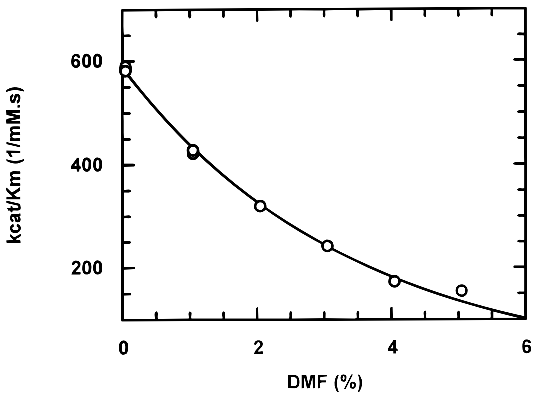

FIGURE 1: Effect of DMF on the activity of oligopeptidase B. The rate constants were determined in the standard buffer, pH 8.0, under first-order conditions with Bz-Arg-Nan substrate, using enzyme concentrations of 18.8−37.6 nM. The solid line represents single-exponential decay.

exponential decay. The magnitude of inhibition is not significantly affected by the addition of 1.0 M NaCl (not shown). The inhibition is somewhat less efficient with dioxane and, in particular, acetonitrile. Therefore, organic solvents were omitted from the reaction mixtures used for the determination of kinetic parameters (see Experimental Procedures).

Irregular pH Dependence. Because oligopeptidase B hydrolyzes the peptide bond at lysine and arginine residues (*7*), a comparison of its kinetic behavior to that of trypsin is of particular interest. The acylation of both chymotrypsin and trypsin is dependent upon two groups, one with a pK_a of about 7 and the other with a pK_a of ∼9 (chymotrypsin) or ∼10 (trypsin) (for reviews see, refs *17*−*19*). The former group corresponds to the catalytically competent histidine residue; the latter is not directly involved in the catalysis, instead it contributes to the stabilization of the active-site structure. In the simplest case, as observed with subtilisin, a sigmoidal curve is obtained, which only depends on ionization of the catalytically competent histidine residue (*20*).

The pH dependence of k_{cat}/K_m usually provides pK_a values that pertain to the free reactant state (*19*, *21*, *22*). Hence, the pK_a for the same enzyme is expected to be independent of the substrate used, provided that the same reaction step is rate-limiting at all pH values (*21*, *22*), as indeed observed in the trypsin and chymotrypsin reactions. Since k_{cat}/K_m is the second-order acylation constant, it is not affected by changes in the ratio of the rate of acylation and deacylation, unlike k_{cat} in the hydrolysis of esters and amides by chymotrypsin.

In contrast to the chymotrypsin reactions, the pH−k_{cat}/K_m profile for oligopeptidase B is significantly dependent on the nature of the substrate, as is evident from the difference between the pK_1 values for the ester and amide substrates (Table 1). The value of pK_1 which is close to 7 reflects the dissociation of the catalytically competent histidine residue. Nevertheless, pK_1 may not be a true dissociation constant, also called microscopic or group constant, but it most probably represents a molecular or macroscopic constant, involving contributions from changes with pH in the rate-determining step and/or from overlapping ionization of some other group (*22*, *23*). This offers an explanation for the different pK_a values found with different substrates. In the case of chymotrypsin and subtilisin, the kinetic pK_a of about 7 is the true dissociation constant of the catalytic histidine, as demonstrated by NMR titration (*24*).

Besides the variation in the pK_1 value, the pH−rate profile is also affected by the reaction conditions. The ionization of some enzymic group causes significant deviation from the simple bell-shaped curve in the reactions with Bz-Arg-Nan and Bz-Arg-Nap at low ionic strength. This complex pH dependence can be approximated by eq 2 involving an unknown ionizing group with an apparent pK_a of ∼8.3 (Figures 2 and 3, Table 1). When this group becomes deprotonated with increasing pH, the protein obtains a net negative unit charge, i.e., it either loses a positive charge or acquires a negative one. This leads to a decrease in catalytic activity, as indicated by the lower k_{cat}/K_m(limit)$_2$ value with respect to k_{cat}/K_m(limit)$_1$. Electrostatic shielding upon addition of 1.0 M NaCl virtually eliminates the effect of the ionizing group, giving rise to a normal bell-shaped curve, so that the activity of the protonated form decreases and that of the unprotonated form increases depending on the pH (Figure 2a). Similar results were obtained with Bz-Arg-Nap, as seen in Figure 2b, where the contributions by the two enzyme forms are also illustrated.

In the case of Bz-Arg-NH_2 (Figure 2c) and, in particular, Bz-Arg-Et (Figure 2d), deviation from the bell-shaped profile is not significant. Addition of salt inhibits the enzyme over the entire pH range. Possibly, the large aromatic groups at the P1′ position render the nitroanilide and the naphthylamide substrates more sensitive to the unknown ionizing group.

The pK_a of 9.7−9.8 found in the reactions of the arginine substrates may reflect ionization of a catalytically influential tyrosine or lysine residue, and this process is most likely accompanied by conformational changes. This is supported by the study of the pH dependence of intrinsic fluorescence, which has indicated that unfolding of the protein occurs above pH 8.5 (*12*). The unfolding is completely reversible at least up to pH 9.5, as demonstrated by activity measurements (*12*).

The origin of the modifying group with the apparent pK_a of ∼8.3 is yet to be established. A thiol group could be a potential candidate. However, this possibility is not supported by abolishing the dissociation of the accessible thiols by blocking with iodoacetamide since the complex character of the pH−rate profile for the Bz-Arg-Nan reaction has not changed (not shown). Hence, the lower activity form of oligopeptidase B in the high-pH region may not be attributed to the ionization of a cysteine residue.

Hydrolysis of Bz-Cit-Et. The importance of the positive charge on the arginine side chain can be tested by using the neutral, structurally similar citrulline derivative. In the case of papain, the k_{cat}/K_m values are similar with Bz-Arg-Et and Bz-Cit-Et, differing by a factor of only 2 (*25*). For the trypsin reaction where, in contrast to papain catalysis, the arginine side chain of the substrate binds to a charged aspartate residue, the rate constant with Bz-Arg-Et is higher by several orders of magnitude than that found with Bz-Cit-Et. In the case of oligopeptidase B, the 3 orders of magnitude difference (Table 1) clearly indicates that the positive charge on the arginine derivatives is crucial for introducing high specificity.

Not only are the rate constants very different with the Bz-Arg-Et and Bz-Cit-Et reactions, but so are the pH−rate

Table 1: Kinetic Parameters for Reactions of Oligopeptidase B[a]

parameters	Bz-Arg-Nan	Bz-Arg-Nap	Bz-Arg-NH_2	Bz-Arg-Et	Bz-Cit-Et
No NaCl					
$k_{cat}/K_m(\text{limit})_1$ ($mM^{-1}s^{-1}$)	1040 ± 75	960 ± 162	334 ± 16 (295 ± 12)[b]	116 ± 25	1.20 ± 0.20
$k_{cat}/K_m(\text{limit})_2$ ($mM^{-1}s^{-1}$)	296 ± 77	343 ± 60	106 ± 31		
pK_1	7.36 ± 0.07	7.41 ± 0.18	7.30 ± 0.06 (7.16 ± 0.07)[b]	6.82 ± 0.03	6.62 ± 0.13
pK_2	8.25 ± 0.18	8.00 ± 0.30	8.47 ± 0.18		7.19 ± 0.12
pK_3	9.77 ± 0.26	9.79 ± 0.16	9.83 ± 0.34 (9.08 ± 0.05)[b]	9.19 ± 0.04	
1.0 M NaCl					
$k_{cat}/K_m(\text{limit})$ ($mM^{-1}s^{-1}$)	571 ± 5.5	597 ± 20	144 ± 4.2	502 ± 11	1.43 ± 0.21[c]
pK_I	6.94 ± 0.02	6.96 ± 0.06	6.90 ± 0.06	6.65 ± 0.04	6.44 ± 0.11[c]
pK_{II}	9.83 ± 0.02	9.70 ± 0.08	9.73 ± 0.08	9.67 ± 0.05	6.81 ± 0.12[c]
$k_{cat}/K_m(\text{limit})_2$ ($mM^{-1}s^{-1}$)					0.082 ± 0.011[c]

[a] The enzyme concentrations were 18.8−75.2 nM for the arginine substrates and 6.6 μM for Bz-Cit-Et. [b] Parameters for a bell-shaped curve. [c] From eq 3.

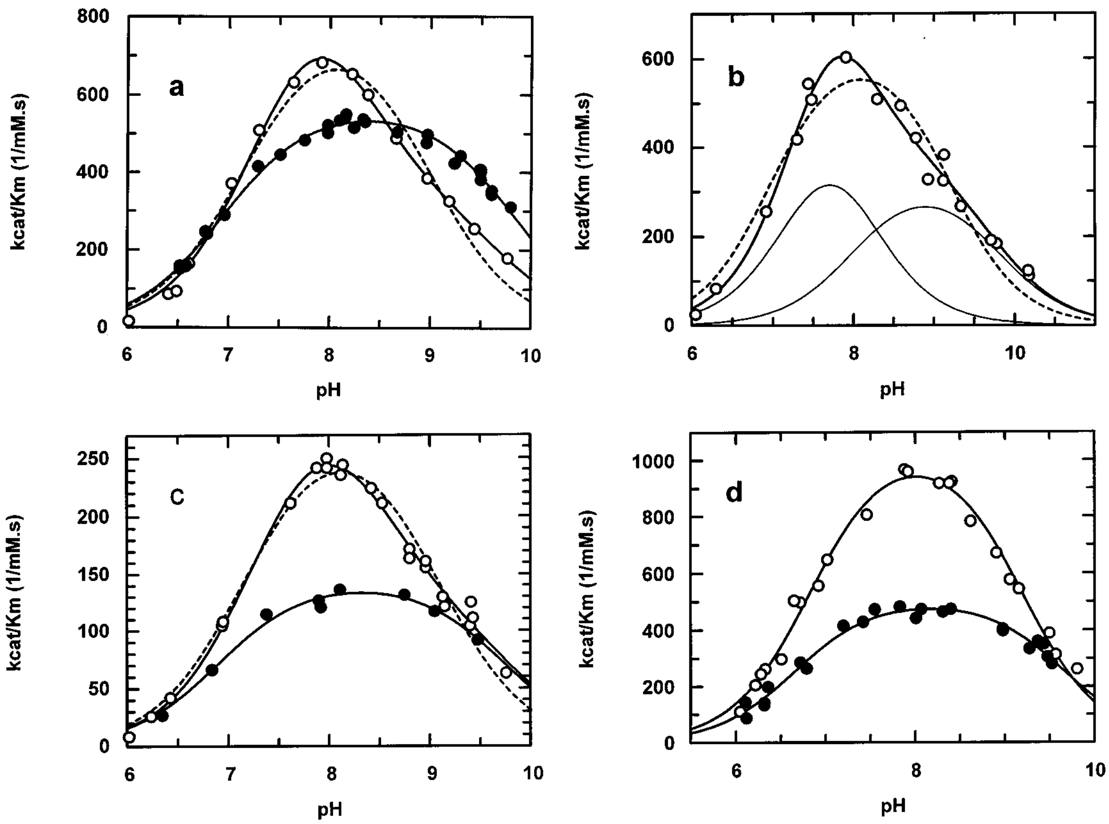

FIGURE 2: pH−k_{cat}/K_m profiles for oligopeptidase B reactions. The substrate and enzyme concentrations were 4.6 μM and 18.8−75.2 nM, respectively, in the absence (○) and presence (●) of 1.0 M NaCl. (a) Hydrolysis of Bz-Arg-Nan. The open circles conform to eq 2, whereas the full points fit to eq 1. The broken line is a bell-shaped curve (eq 1) fitted to the open circles. (b) Hydrolysis of Bz-Arg-Nap. The broken line is a bell-shaped curve (eq 1) fitted to the points. The thin lines represent the two active components of the enzyme. (c) Hydrolysis of Bz-Arg-NH_2. (d) Hydrolysis of Bz-Arg-Et.

profiles. The reaction of Bz-Arg-Et displays a wide optimum pH not significantly perturbed by the ionization of an enzymatic group, whereas the Bz-Cit-Et reaction gives an unexpectedly narrow bell-shaped profile, confined to the lower pH region (Figure 3). The occurrence of two pK_a values on opposite sides of the very sharp bell-shaped curves reveals a kinetically influential ionizing group of pK_a close to 7, in addition to the catalytically competent histidine residue.

Assigning the two close pK_a values (6.62 and 7.19) to the respective ionizing groups is rather difficult. At first sight, it may appear that the lower pK_a belongs to the lower limb of the curve and represents ionization of the catalytic histidine whereas the higher pK_a relates to a general acid. However, the opposite is equally possible as is evident from a series of bell-shaped curves generated with a constant $pK_I = 7.00$ and a variety of pK_{II} values (Figure 4). As shown by the broken line in the model of Figure 4, the pK_a of the general acid may indeed be lower ($pK_{II} = 6.00$) than that of the general base ($pK_I = 7.00$). This might be the case with the citrulline derivative (Figure 3) since it is the higher pK_a which is closer to the pK_a of the catalytic histidine found with the other substrates.

Dissociation of a proton with increasing pH from the general acid virtually eliminates the catalytic competence of the enzyme, but some activity remains in the presence of 1.0 M NaCl (Figure 3 and Table 1). The effect of this group, which is important in the reactions of Bz-Cit-Et, becomes

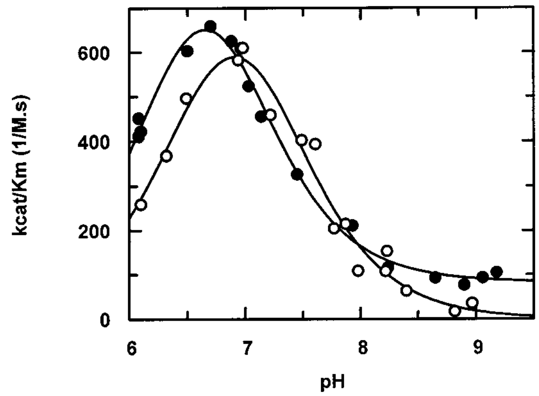

FIGURE 3: pH−k_{cat}/K_m profile of the hydrolysis of Bz-Cit-Et by oligopeptidase B. The enzyme concentration was 3.3−13.3 μM. The points are as in Figure 2. The open and full circles were fitted to eqs 1 and 3, respectively.

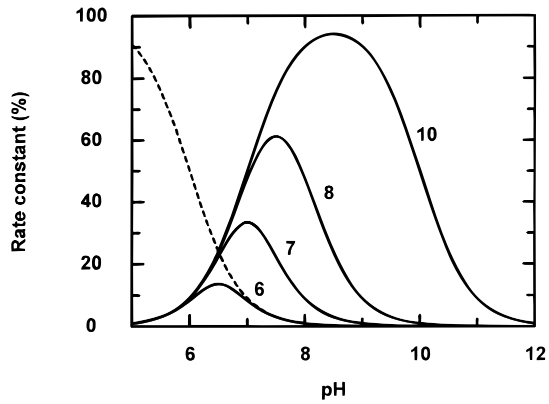

FIGURE 4: pH−rate profiles calculated by using eq 1 with a limiting rate constant of 100, pK_I = 7.00, and for values of pK_{II} indicated in the figure. The broken line shows the ionization of an acid with pK_a = 6.00.

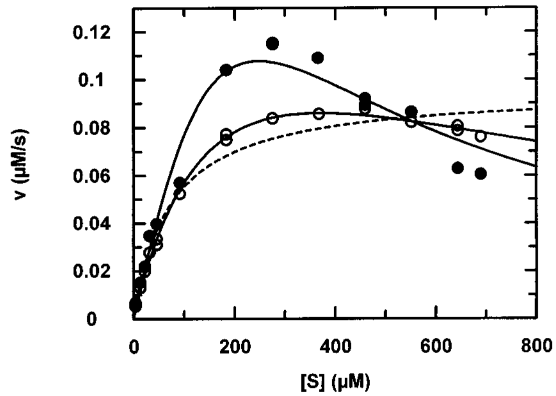

FIGURE 5: Reaction rates plotted against substrate concentration. (○) The initial rates were measured in standard buffer, pH 7.10. The points fit to eq 4 representing substrate inhibition (solid line) but not to the simple Michaelis−Menten kinetics (broken line). (●) The reactions were carried out in standard buffer, pH 8.10, containing 1.0 M NaCl. The points do not fit to the solid line derived from eq 4 (k_{cat} = 613 s^{-1}, K_m = 1240 μM, K_i = 50 μM).

negligible in the case of arginine substrates, where a strong interaction between the enzyme and substrate enhances the catalytic activity by 3 orders of magnitude. Indeed, the K_i value of eq 5, which may be equal to K_s (see next paragraph), is much higher for Bz-Cit-Et than for Bz-Arg-Et. However, the true K_i value could not be determined because of the poor solubility of the citrulline compound. The substantial difference in the rate constants suggests that the arginine substrates bind to an enzymic carboxylate ion, whereas the citrulline compound assumes a less favorable alternative position.

Substrate Inhibition. The K_m values were determined with initial rate measurements. Figure 5 clearly illustrates that the Michaelis−Menten kinetics breaks down in the hydrolysis of Bz-Arg-Nan. The decrease in rate with increasing substrate concentration can be explained in terms of substrate inhibition. The inhibitory effect by a second molecule of the same substrate is evident from the adherence of data to eq 4 in the absence of NaCl. The Michaelis parameters and the dissociation constants for the inhibitory substrate are shown in Table 2. If 1.0 M NaCl is added to the reaction mixture, the data no longer fit to the theoretical curve derived from eq 4 (Figure 5), so that correct constants may not be calculated. The complexity of substrate inhibition may be associated with structural changes and/or electrostatic shielding of some ionizing groups in the presence of elevated salt concentration. The remarkable substrate inhibition distinguishes oligopeptidase B from trypsin, subtilisin, and even the structurally related prolyl oligopeptidase. Substrate inhibition has also been found with Bz-Arg-Nap (Table 2). No such inhibition could be observed with Bz-Arg-NH_2 and Bz-Arg-Et because the substantial background absorbance at 253 nm did not permit us to use a sufficiently high concentration of substrate.

Utilizing the inhibitory effect of poor substrates on the hydrolysis of highly specific substrates (*26*), we have determined the $K_i \approx K_s$ value for Bz-Arg-NH_2 and Bz-Arg-Et where substrate inhibition is negligible. These substrates are good inhibitors of Z-Arg-Arg-Amc, allowing one to calculate K_i values with eq 5. In contrast, the nitroanilide and naphthylamide derivatives exhibit substrate inhibition under the measurement conditions, and this may interfere with the determination. It is seen in Table 2 that the K_i data are lower than the K_m values for Bz-Arg-NH_2 and Bz-Arg-Et. This indicates that K_m does not represent the binding constant for these substrates and suggests that a conformational change rather than the chemical step is rate-limiting in acylation. The $K_i \approx K_s$ values for Bz-Arg-NH_2 and Bz-Arg-Et do not appreciably differ, and the values moderately increase with increasing pH.

Substrate inhibition was also found with Z-Arg-Arg-Amc (*8*). However, K_m for this substrate was lower by 2 orders of magnitude (Table 2). Hence, the high specificity of Z-Arg-Arg-Amc relies upon tighter binding. Such a great increase in binding energy between enzyme and substrate suggests that the side chain of the second arginine is matched by a carboxylate ion of the enzyme or at least the charged guanidinium ion of the side chain forms a strong hydrogen bond with a main chain CO or some side chain. It should be noted that the extension of the substrate backbone is not responsible for the large increase in k_{cat}/K_m since the rate constant for Z-Phe-Arg-Amc is 1.4 μM^{-1} s^{-1} compared with 63 μM^{-1} s^{-1} for Z-Arg-Arg-Amc. The importance of the positive charge on the Arg at the P2 position is also supported by the decrease of 1 order of magnitude in the rate constant in the presence of 1.0 M NaCl (*8*). The strong binding implies that the second arginine residue stabilizes the enzyme−substrate complex and the transition state to a similar extent, which results in better binding without affecting k_{cat}. In

Table 2: Michaelis–Menten Parameters for Reactions of Oligopeptidase B[a]

substrate	pH	k_{cat} (s^{-1})	K_m (μM)	K_{is} (μM)	K_i[b] (μM)
Bz-Arg-Nan	7.10	91.6 ± 6.7	195 ± 21	698 ± 105	
Bz-Arg-Nan	8.03	188.2 ± 48.7	269 ± 96	354 ± 146	
Bz-Arg-Nan[c]	8.00	114.2 ± 19.0	301 ± 70	470 ± 136	
Bz-Arg-Nap	8.02	80.8 ± 14.6	97 ± 28	282 ± 85	
Z-Arg-Arg-Amc[d]	7.78	37.7 ± 2.1	1.02 ± 0.15	21.1 ± 3.4	
Bz-Arg.NH_2[e]	6.90		>1000		436 ± 24
Bz-Arg-NH_2[e]	7.97		>1000		488 ± 13
Bz-Arg-Et[e]	7.05		>800		312 ± 6.9
Bz-Arg-Et[e]	8.00		>800		398 ± 14
Bz-Arg-Et[e]	9.10		>800		537 ± 32

[a] Measured with 2.2 nM enzyme at 25 °C in standard buffer. [b] Calculated from eq 5. [c] Measured at 37 °C. [d] From ref 8. [e] In the presence of 1.0 M NaCl.

Table 3: Kinetic Deuterium Isotope Effects[a]

substrate	no NaCl	1.0 M NaCl
Bz-Arg-Nan	0.91	1.44
Bz-Arg-Nan		1.53[b]
Bz-Arg-Nan		1.41[c]
Bz-Arg-NH_2	0.99	1.47
Bz-Arg-Et	0.62	1.13
Bz-Cit-Et		1.12

[a] The ratio of the rate constants, $k_{cat}/K_m(H_2O)/k_{cat}/K_m(^2H_2O)$, were calculated with the maximum value of each pH-dependence curve at 25.0 °C. [b] Determined at 39.1 °C. [c] Determined at 10.1 °C.

contrast, with the extensively studied peptidases, the binding energy of an extended substrate does not lower K_m but enhances k_{cat} and thus k_{cat}/K_m (*27*). In this case, the incremental binding energy is used for stabilization of the transition state.

Composite Transition State for the Rate-Limiting Step. The study of kinetic deuterium isotope effects has proved to be conducive to the mechanistic investigations of serine peptidases. Such studies have revealed that the catalysis proceeds slower in heavy water by a factor of 2–3, indicating that the rate-limiting step of the reaction involves general acid/base catalysis (cf. *17*, *18*). General base and general acid catalyses, respectively, promote the formation and decomposition of the tetrahedral intermediate, the obligatory species on the reaction pathway of peptidases. Unlike the rate constants of the trypsin and chymotrypsin reactions, the second-order acylation rate constant (k_{cat}/K_m) for oligopeptidase B does not exhibit the expected isotope effect of 2–3 in the absence of salt but rather $k_{cat}/K_m(H_2O)/k_{cat}/K_m(^2H_2O)$ is near unity or shows an appreciably inverse effect (Table 3). The origin of the inverse isotope effects is not clear. It may arise from the strengthening of the hydrogen bond during the rate-limiting isomerization discussed below (eq 8). Upon addition of 1.0 M NaCl, $k_{cat}/K_m(H_2O)/k_{cat}/K_m(^2H_2O)$ is above unity, indicating some contribution by general acid/base catalysis.

The principal contribution to the rate-limiting transition state may come from a physical process. In the absence of salt, the reaction is entirely controlled by the physical step, which is presumably isomerization of the enzyme–substrate complex (ES ↔ E′S) shown in eq 8, which depicts the minimal mechanism of the acylation step. E′S ↔ ET and ET ↔ EA represent the general base-catalyzed formation of the tetrahedral intermediate and its general acid-catalyzed decomposition to acyl–enzyme, respectively. Hence, it can be concluded that in the absence of salt, the rate-limiting

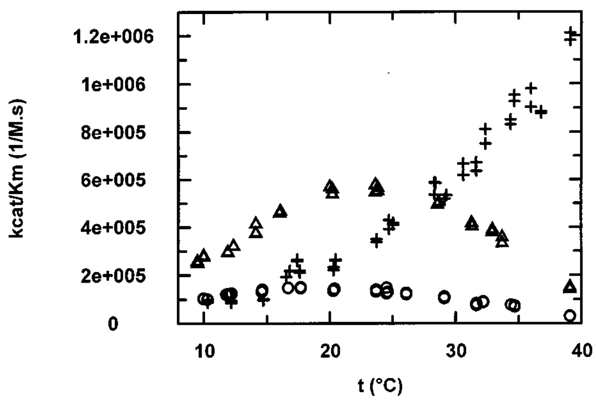

FIGURE 6: Temperature dependence of k_{cat}/K_m for the hydrolysis of Bz-Arg-Nan (△), Bz-Arg-NH_2 (○), and Bz-Arg-Et (+) by oligopeptidase B. The reactions were measured under first-order conditions in 3.0 mL standard buffer, pH 8.0, containing 1.0 M NaCl. The buffer in the cell was equilibrated at the appropriate temperature before the addition of 10 μL enzyme, which yielded a 10–40 nM final enzyme concentration.

transition state involves an isomerization step, while at 1.0 M NaCl, both the isomerization and the general base catalysis contribute to the transition state.

$$E + S \leftrightarrow ES \leftrightarrow E'S \leftrightarrow ET \leftrightarrow EA \qquad (8)$$

The involvement of a physical rather than a chemical step in the rate-limiting transition state is consistent with the rate constant found with Bz-Arg-Et. Having a relatively good leaving group, esters exhibit much higher chemical reactivity than amides (*18*, *19*). Indeed, Bz-Arg-Et is fairly well hydrolyzed at alkaline pH, say at pH 10, where the corresponding amides are quite stable. A similar reactivity difference is also found in the chymotrypsin catalysis. In contrast, oligopeptidase B hydrolyzes the two types of substrate with similar k_{cat}/K_m values (Table 1), indicating that the substantial reactivity difference is not manifested in the rate-limiting transition state.

Unusual Temperature Sensitivity of the Catalysis. Enzymatic reaction rates commonly increase with a rise in temperature to 37 °C or even higher, provided that the structure of the reacting enzyme is stable. Unexpectedly, the rate constant for the reactions of oligopeptidase B with Bz-Arg-Nan and Bz-Arg-NH_2 tend to diminish above ~25 °C (Figure 6), although after incubation at 38 °C the enzyme exhibits full activity at 25 °C. The reactions were measured in the presence of 1.0 M NaCl, where the pH optimum was appreciably broader. It is important that the structure of

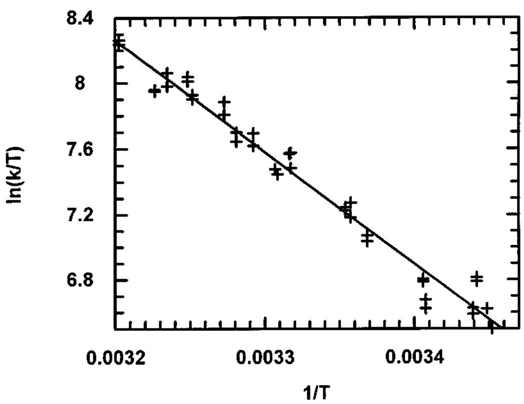

FIGURE 7: Eyring plot of the reaction of Bz-Arg-Et with oligopeptidase B. The linear fit for the points between 16.5 and 39.1 °C gave $\Delta H^* = 56.6$ kJ·mol^{-1} and $\Delta S^* = 52.4$ J·K^{-1}·mol^{-1}.

oligopeptidase B is virtually unchanged when the temperature was raised from 25 to 38 °C and tested by the sensitive near-UV CD method (*12*). However, a delicate alteration in the structure cannot be excluded. Furthermore, the decline in activity may not be attributed to weaker binding because of the change in k_{cat} rather than in K_m (Table 2).

Surprisingly, the reaction of Bz-Arg-Et exhibits an ordinary temperature dependence in the upper temperature range (Figure 6). This indicates that a significant structural alteration should not occur with increasing temperature. The ester substrate is devoid of the hydrogen atom in the leaving group that is present in amides. The amide hydrogen presumably forms a hydrogen bond with the enzyme at low temperature, but the bond strength weakens with increasing temperature. This effect, of course, cannot interfere with hydrolysis of the ester substrate at high temperature.

It is clear from Figure 6 that a linear Eyring plot (ln[k/T] vs 1/T) cannot be obtained for the reactions of Bz-Arg-Nan and Bz-Arg-NH_2 in the temperature range of 10−38 °C. Deviation from linearity often arises from a change with temperature in the rate-limiting step (*28*). However, this possibility is not supported by kinetic deuterium isotope effects, which are identical within experimental error at 18.1, 25.0, and 39.1 °C (Table 3). Furthermore, the temperature dependence of k_{cat}/K_m for the reactions of Bz-Arg-Nan and Bz-Arg-NH_2 is similar to that obtained with the most specific Z-Arg-Arg-Amc substrates (not shown).

Linear Eyring plots were obtained for the lower temperature range of the Bz-Arg-Nan reaction (9.5−16.0 °C) and for the Bz-Arg-Et hydrolysis between 16.5 and 39.1 °C (Figure 7). For enzyme reactions the transition state is usually more ordered than the ground state, and this leads to a negative entropy of activation. In contrast, with oligopeptidase B, both plots resulted in marked positive ΔS^*, namely 66.2 and 52.4 J·K^{-1}·mol^{-1}, respectively, which were compensated for by large ΔH^* values. Positive ΔS^* could be coupled with reorganization of the protein structure (*28*), which may involve an unfolding process or changes in the water layer around the reactants. Isomerization and solvent reorganization in the rate-limiting step can account for the positive activation entropy and the lack of normal kinetic solvent isotope effect. The importance of water molecules at the active site is consistent with the high sensitivity of oligopeptidase B to organic solvents.

It has been known that mutations may lead to protein variants which display low activity at 37 °C relative to the wild-type enzyme, but the activity is apparently not impaired at 30−32 °C. Such temperature-sensitive variants have been identified, for example, in the case of bacteriophage T4 lysozyme (*29*, *30*) and human immunodeficiency virus type 1 protease (*31*). Oligopeptidase B is different from these enzymes as it is a naturally occurring enzyme and its temperature sensitivity is substrate dependent. Such a phenomenon is observed for the first time.

Conclusion. Oligopeptidase B, an enzyme implicated in serious disease states, differs in several respects from other serine peptidases. It exhibits irregular pH−rate profiles for several substrates, which may arise from the ionization of some surface groups not directly involved in the chemical reaction. The pK_a characteristic of the catalytic histidine is not a microscopic constant, it is affected by the overlapping ionization, giving rise to the different pK_a values in the reactions of ester and amide substrates.

The rate-limiting step of the oligopeptidase B catalysis is a conformational change in the absence of salt, rather than general acid/base catalysis found with the trypsin- and subtilisin-like enzymes. In the presence of 1.0 M NaCl, the rate-limiting transition state involves both physical and chemical components. A surprising feature of oligopeptidase B concerns its temperature sensitivity to the amide but not to the ester substrates. An interaction between the NH group of the P1′ residue and an enzymic group may be responsible for this phenomenon and for the variation in the pK_a and kinetic isotope effects.

Binding of arginine substrates to enzymic carboxylate ions is essential for specific catalysis, as is evident from the slow hydrolysis of the isosteric citrulline substrate. Furthermore, the dramatic change in the pH−rate profile of the Bz-Cit-Et reaction indicates different binding modes for this substrate with respect to Bz-Arg-Et. The high kinetic specificity of oligopeptidase B toward Z-Arg-Arg-Amc is manifested in a tight substrate binding rather than in a more effective transition-state stabilization, the major factor in lowering the activation energy of extended substrate reactions with trypsin-like peptidases.

The mechanistic features which distinguish oligopeptidase B from the human serine peptidases may facilitate drug design to counteract cell invasion by trypanosomes.

ACKNOWLEDGMENT

Thanks are due to Ms. J. Fejes and Ms. I. Szamosi for excellent technical assistance.

REFERENCES

1. Rawlings, N. D., Polgár, L., and Barrett, A. J. (1991) *Biochem. J. 279*, 907−908.
2. Polgár, L. (1992) *FEBS Lett. 131*, 281−284.
3. Polgár, L. (1994) *Methods Enzymol. 244*, 188−200.
4. Fülöp, V., Böcskei, Z., and Polgár, L. (1998) *Cell 94*, 161−170.
5. Kanatani, A., Masuda, T., Shimoda, T., Misoka, F., Xu, L.-S., Yoshimoto, T., and Tsuru, D. (1991) *J. Biochem. (Tokyo) 110*, 315−320.
6. Barrett, A. J., and Rawlings, N. D. (1992) *Biol. Chem. Hoppe-Seyler 373*, 553−560.
7. Tsuru, D., and Yoshimoto, T. (1994) *Methods Enzymol. 244*, 201−215.

8. Polgár, L. (1997) *Proteins: Struct. Funct. Genet. 28*, 375−379.
9. Kahyaoglu, A., Haghjoo, K., Frank, J., Kettner, C., Felföldi., F., and Polgár., L. (1997) *J. Biol. Chem. 272*, 25547−25554.
10. Burleigh, B. A., Caler, E. V., Webster, P., and Andrews, N. W. (1997) *J. Cell. Biol. 136*, 609−620.
11. Caler, E. V., de Avalos, S. V., Haynes, P. A., Andrews, N. W., and Burleigh, B. A. (1998) *EMBO J. 17*, 4975−4986.
12. Polgár, L., and Felföldi, F. (1998) *Proteins: Struct. Funct. Genet. 30*, 424−434.
13. Leatherbarrow, R. J. (1990) *GraFit, Version 2.0,* Erithacus Software Ltd. Staines, U.K.
14. Dixon, M., and Webb, E. C. (1979) in *Enzymes* (Dixon, M., Webb, E. C., Thorne, J. C. R., and Tipton, K. F.) 3rd ed., pp 126−138, Elsevier Science, Amsterdam.
15. Glassoe, P. K., and Long, F. A. (1960) *J. Phys. Chem. 64*, 188−190.
16. Ellman, G. L. (1959) *Arch. Biochem. Biopphys. 82*, 70−77.
17. Polgár, L. (1987) *New Comp. Biochem. 16*, 159−200.
18. Polgár, L. (1989) *Mechanisms of Protease Action,* pp 87−122, CRC Press, Boca Raton, FL.
19. Bender, M. L., and Kézdy, F. J. (1965) *Annu. Rev. Biochem. 34*, 49−76.
20. Polgár, L., and Fejes, J. (1979) *Eur. J. Biochem. 102*, 531−536.
21. Fersht, A. (1985) *Enzyme structure and mechanism,* 2nd ed., pp 155−175, W. H. Freeman and Co., New York.
22. Brocklehurst, K. (1994) *Protein Eng. 7*, 291−299.
23. Dixon, H. B. F., Clarke, S. D., Smith, G. A., and Carne, T. K. (1991) *Biochem. J. 278*, 279−284.
24. Jordan, F., Polgár; L., and Tous, G. (1985) *Biochemistry 24*, 7711−7717.
25. Asbóth, B., and Polgár, L. (1977) *Acta Biochim. Biophys. Acad. Sci. Hung. 12*, 329−333.
26. Asbóth, B. and Polgár, L. (1983) *Biochemistry 22*, 117−122.
27. Fersht, A. (1985) *Enzyme structure and mechanism*, 2nd edition, pp 311−346, W. H. Freeman and Co., New York.
28. Laidler, K. J., and Peterman, B. F. (1979) *Methods Enzymol. 63*, 234−257.
29. Alber, T., Dao-Pin, S., Nye, J., Muchmore, D., and Matthews, B. (1987) *Biochemistry 26*, 3754−3758.
30. Gray, T. M., and Matthews, B. W. (1987) *J. Biol. Chem. 262*, 16858−16864.
31. Manchester, M., Everitt, L., Loeb, D. D., Hutchison, C. A., III, and Swanstrom, R. (1994) *J. Biol. Chem. 269*, 7689−7695.

BI991767A